Second-Order Heterogeneous Multi-Agent Target Tracking Without Relative Velocities

Cristian F. Nino, *Graduate Student Member, IEEE*, Omkar Sudhir Patil, and Warren E. Dixon, *Fellow, IEEE*

***Abstract*—The multi-agent target tracking problem has received growing interest in the robotics and controls community in recent years. In particular, distributed target tracking is an abstraction for many potential applications. However, typical results assume that full state information is available. This letter addresses the multi-agent target tracking problem, where only the relative distance between neighbors is known. To yield this result, a novel distributed observer is designed that employs an auxiliary distributed filter. The distributed observer achieves network-to-target regulation by enabling the network of agents to estimate the relative velocities of all agents and the target. The distributed filter/observer structure is motivated by a Lyapunov-based stability analysis, which is provided to ensure that all agents are exponentially regulated to a neighborhood of the target. Comparative simulations are provided to demonstrate the performance of the developed method. The simulation results indicate that six agents modeled by an unknown heterogeneous damped and driven harmonic oscillator can successfully track a target agent. The developed method provides a 67% improvement in the RMS tracking error when compared to a baseline.**

***Index Terms*—Multi-agent systems, output feedback control, Lyapunov methods, nonlinear control systems.**

I. Introduction

MULTI-AGENT systems have witnessed significant advancements in distributed guidance, navigation, and control in recent years [1]. In particular, second-order multi-agent target tracking has gained prominence due to its versatility in modeling various real-world scenarios [2]. Examples of distributed second-order systems that facilitate a tracking objective include manipulator robots, aircraft, and spacecraft [3], [4], [5], [6], [7].

Manuscript received 8 September 2023; revised 14 November 2023; accepted 29 November 2023. Date of publication 7 December 2023; date of current version 22 December 2023. This work was supported in part by the Air Force Office of Scientific Research (AFOSR) under Grant FA9550-19-1-0169; in part by the Air Force Research Laboratory (AFRL) under Grant FA8651-21-F-1027; and in part by the Office of Naval Research under Grant N00014-21-1-2481. Recommended by Senior Editor J. Daafouz. *(Corresponding author: Cristian F. Nino.)*

The authors are with the Department of Mechanical and Aerospace Engineering, University of Florida, Gainesville, FL 32611 USA (e-mail: cristian1928@ufl.edu; patilomkarsudhir@ufl.edu; wdixon@ufl.edu).

Digital Object Identifier 10.1109/LCSYS.2023.3340237

In the context of autonomous robotics, the prevailing methods for developing distributed tracking control strategies heavily rely on the type and quality of information that is available. One of the most commonly used assumptions is the access of full state information, which includes the availability of relative velocity measurements. However, relative velocity measurements may not be accessible or accurate in various robotics applications [8]. Thus, it is desirable to develop methods that rely solely on relative position information, eliminating the need for a common reference frame and allowing for on-board computation using sensors like cameras or ultrasonic sensors.

Motivated to eliminate full state feedback, the result in [9] addressed the multi-agent tracking problem in the context of leader-follower consensus, where the tracked leader has unmeasurable velocity states. However, the follower agents are assumed to have a first-order dynamic model; thus, the result does not address the problem of relative velocity measurements. Second-order dynamics were later considered, but relative velocity measurements were still assumed to be known [10]. This limitation is addressed in [11], [12], [13], [14] by incorporating a linear second-order dynamic model for agents and constructing a distributed observer. Subsequent results, notably [15] and [16], further expanded upon these ideas to incorporate heterogeneous dynamics. However, all of the aforementioned results do not account for nonlinearity in the dynamics, which can deteriorate the stability and performance of the closed-loop system.

The result in [17] examines the leader-follower second-order consensus problem, without the use of velocity measurements for nonlinear systems. The authors developed an observer-based output-feedback controller based on the non-separation principle [18]. This approach requires that both the homogeneous network agents and the tracked agent operated under identical drift dynamics, which limits the generality and application of their results.

In this letter, a distributed observer is developed to address the target tracking problem for a network of agents with unknown heterogeneous second-order nonlinear dynamics without relative velocity measurements. The distributed observer design is facilitated by constructing an auxiliary distributed filter using only the relative positions. As a result, the developed observer estimates relative velocities of the target agent and the controlled agents. A Lyapunov-based analysis is used to guarantee that all agents are exponentially regulated to a neighborhood of the target. To demonstrate the efficacy and performance of the developed method, comparative simulations are provided for a network of six agents, where the method in [17] is used as the baseline. The simulation results show that the developed method provides a 67% improvement in the RMS tracking error.

II. Notation and Preliminaries

The $p\times p$ identity matrix and the $p\times 1$ column vector of ones are denoted by I_p and 1_p, respectively. Given $M \in \mathbb{Z}_{>0}$, the enumeration operation $[\cdot]$ is defined as $[M] \triangleq \{1, 2, \ldots, M\}$. The Kronecker product of $A \in \mathbb{R}^{p\times q}$ and $B \in \mathbb{R}^{m\times n}$ is denoted by $A \otimes B \in \mathbb{R}^{pm\times qn}$. The block diagonal matrix whose diagonal blocks consist of $G_1, G_2, \ldots, G_n$ is denoted by $\mathrm{diag}(G_1, G_2, \ldots, G_n)$. The maximum and minimum eigenvalues of G are denoted by $\lambda_{\max}(G) \in \mathbb{R}$ and $\lambda_{\min}(G) \in \mathbb{R}$, respectively. Given a positive integer N and collection $\{x_i\}_{i\in[N]} \subset \mathbb{R}^n$, let $(x_i)_{i\in[N]} \triangleq [x_1^\top, x_2^\top, \ldots, x_N^\top]^\top \in \mathbb{R}^{nN}$.

Let $\mathcal{G} \triangleq (\mathcal{V}, \mathcal{E})$ represent a static and undirected graph with number of nodes $N \in \mathbb{Z}_{\geq 2}$, node set $\mathcal{V} \triangleq [N]$, and edge set $\mathcal{E} \subseteq \mathcal{V} \times \mathcal{V}$. The edge $(i, k) \in \mathcal{E}$ if and only if node i can send information to node k. Since the graph $\mathcal{G}$ is undirected, $(i, k) \in \mathcal{E}$ if and only if $(k, i) \in \mathcal{E}$. An undirected graph is connected whenever there exists a sequence of edges in $\mathcal{E}$ linking any two distinct nodes. The neighborhood set of node i is $\mathcal{N}_i \triangleq \{k \in \mathcal{V}\backslash\{i\} : (k, i) \in \mathcal{E}\}$. Let $\mathcal{A} \triangleq [a_{ik}] \in \mathbb{R}^{N\times N}$ be the adjacency matrix of $\mathcal{G}$, where $a_{ik} = 1$ if $(k, i) \in \mathcal{E}$ and $a_{ik} = 0$ otherwise. Within this letter, no self-loops are considered. Therefore, $a_{ii} \triangleq 0$ for all $i \in \mathcal{V}$. The degree matrix of $\mathcal{G}$ is $\mathcal{D} \triangleq \mathrm{diag}(\mathcal{A} \cdot 1_N) \in \mathbb{R}^{N\times N}$. Using the degree and adjacency matrices, the Laplacian matrix of the graph $\mathcal{G}$ is $\mathcal{L}_{\mathcal{G}} \triangleq \mathcal{D} - \mathcal{A} \in \mathbb{R}^{N\times N}$.

III. Problem Formulation

Consider a network composed of N agents indexed by $\mathcal{V}$, with a static, connected, and undirected communication graph modeled by $\mathcal{G} \triangleq (\mathcal{V}, \mathcal{E})$, where $\mathcal{E} \subseteq \mathcal{V} \times \mathcal{V}$ denotes the edge set. The model for agent $i \in \mathcal{V}$ is given by

$$\ddot{q}_i = f_i(q_i, \dot{q}_i, t) + u_i, \tag{1}$$

where $q_i, \dot{q}_i, \ddot{q}_i \in \mathbb{R}^n$ denote the generalized position, velocity, and acceleration, respectively, $u_i \in \mathbb{R}^n$ denotes the control input, and $f_i : \mathbb{R}^n \times \mathbb{R}^n \times \mathbb{R}_{\geq 0} \to \mathbb{R}^n$ denotes an unknown locally Lipschitz function in q_i and $\dot{q}_i$, uniformly bounded in t. Consider a target with the stable model

$$\ddot{q}_0 = g(q_0, \dot{q}_0, t), \tag{2}$$

such that $\|q_0\| \leq \bar{q}_0 \in \mathbb{R}_{\geq 0}$ and $\|\dot{q}_0\| \leq \bar{\dot{q}}_0 \in \mathbb{R}_{\geq 0}$, where $q_0, \dot{q}_0, \ddot{q}_0 \in \mathbb{R}^n$ denote the generalized position, velocity, and acceleration, respectively, and $g : \mathbb{R}^n \times \mathbb{R}^n \times \mathbb{R}_{\geq 0} \to \mathbb{R}^n$ denotes an unknown locally Lipschitz function in q_0 and $\dot{q}_0$, uniformly bounded in t. Each agent is capable of measuring only the relative position between itself and its neighbors, which is given by

$$d_{ij} \triangleq q_j - q_i, \forall j \in \mathcal{N}_i. \tag{3}$$

The objective is to develop a distributed controller capable of regulating each agent to the target, based on only the relative position measurement. To quantify the target regulation objective, let the tracking error $e_i \in \mathbb{R}^n$ of agent $i \in \mathcal{V}$ be

$$e_i \triangleq q_0 - q_i. \tag{4}$$

Based on the subsequent stability analysis, we also define the auxiliary tracking error $r_i \in \mathbb{R}^n$ of agent $i \in \mathcal{V}$ as

$$r_i \triangleq \dot{e}_i + k_1 e_i, \tag{5}$$

where $k_1 \in \mathbb{R}_{>0}$ is a user-defined gain. The following section provides the control design to achieve the stated objective.

IV. Control Synthesis

Since at least one agent must be able to measure e_i, we let $b_i \in \{0, 1\}$ denote the indicator of whether an agent $i \in \mathcal{V}$ is capable of measuring e_i. Let the relative position $\eta_i \in \mathbb{R}^n$ and relative velocity $\zeta_i \in \mathbb{R}^n$ be defined as

$$\eta_i \triangleq \sum_{j\in\mathcal{N}_i} d_{ij} + b_i e_i, \tag{6}$$

and

$$\zeta_i \triangleq \dot{\eta}_i = \sum_{j\in\mathcal{N}_i} \dot{d}_{ij} + b_i \dot{e}_i, \tag{7}$$

respectively, for all $i \in \mathcal{V}$.

Define the interaction matrix $\mathcal{H} \triangleq I_n \otimes (\mathcal{L}_{\mathcal{G}} + \mathrm{diag}(b_1, \ldots, b_N)) \in \mathbb{R}^{nN\times nN}$. Using (6) and the definitions of the graph Laplacian and interaction matrix, the relative positions can be expressed in an ensemble form as

$$\eta = \mathcal{H} e, \tag{8}$$

where $\eta \triangleq (\eta_i)_{i\in\mathcal{V}} \in \mathbb{R}^{nN}$ and $e \triangleq (e_i)_{i\in\mathcal{V}} \in \mathbb{R}^{nN}$. Based on (8), the relative velocities can be expressed in an ensemble form as

$$\zeta = \mathcal{H}\dot{e}, \tag{9}$$

where $\zeta \triangleq (\zeta_i)_{i\in\mathcal{V}} \in \mathbb{R}^{nN}$.

Remark 1: Since the communication graph is connected and $b_i \neq 0$ for at least one i, $\mathcal{H}$ is a positive-definite M-matrix. [19, Corollary 4.33].

A. Distributed Observer Development

Since the relative velocities are unknown, we develop a distributed observer that generates estimates of η_i and ζ_i, given by $\hat{\eta}_i, \hat{\zeta}_i \in \mathbb{R}^n$, respectively. The corresponding relative position estimation error $\tilde{\eta}_i \in \mathbb{R}^n$ and the relative velocity estimation error $\tilde{\zeta}_i \in \mathbb{R}^n$ are quantified as

$$\tilde{\eta}_i \triangleq \hat{\eta}_i - \eta_i, \tilde{\zeta}_i \triangleq \hat{\zeta}_i - \zeta_i, \tag{10}$$

respectively, for all $i \in \mathcal{V}$. To facilitate the subsequent development, we introduce the auxiliary estimation error $\tilde{r}_i \in \mathbb{R}^n$ defined as

$$\tilde{r}_i \triangleq \dot{\tilde{\eta}}_i + k_3 \tilde{\eta}_i + \rho_i, \tag{11}$$

for all $i \in \mathcal{V}$, where $k_3 \in \mathbb{R}_{>0}$ is a user-defined gain, and $\rho_i \in \mathbb{R}^n$ denotes the output from a dynamic filter which compensates for the fact that the state ζ_i is not measurable. Based on the subsequent stability analysis, ρ_i is designed as the output of the dynamic filter

$$\dot{\rho}_i \triangleq \tilde{\eta}_i - (k_3 + k_4)\tilde{r}_i - k_5\rho_i,\ \rho_i(t_0) = 0, \tag{12}$$

where $k_4, k_5 \in \mathbb{R}_{>0}$ are user-defined gains. Substituting (11) into (12) and integrating the resulting equation from t_0 to t, (12) is implemented as

$$\rho_i(t) = \left(1 - k_3^2 - k_3k_4\right)\int_{t_0}^{t}\tilde{\eta}_i(\tau)\mathrm{d}\tau - \left(k_3 + k_4 + k_5\right)\int_{t_0}^{t}\rho_i(\tau)\mathrm{d}\tau - (k_3 + k_4)\tilde{\eta}_i(t), \tag{13}$$

for all $i \in \mathcal{V}$. Based on the subsequent analysis, we design the distributed observer as

$$\begin{aligned}\dot{\hat{\eta}}_i &= \hat{\zeta}_i,\ \hat{\eta}_i(t_0) = 0,\\ \dot{\hat{\zeta}}_i &= \sum_{j\in\mathcal{N}_i}\left(u_j - u_i\right) - b_iu_i + (2k_3 + k_4 + k_5)\rho_i\\ &\quad - \left(2 - k_3^2\right)\tilde{\eta}_i,\ \hat{\zeta}_i(t_0) = 0,\end{aligned} \tag{14}$$

for all $i \in \mathcal{V}$. Using the definitions of the graph Laplacian and interaction matrix, (14) can be expressed as

$$\begin{aligned}\dot{\hat{\eta}} &= \hat{\zeta},\\ \dot{\hat{\zeta}} &= -\mathcal{H}u + (2k_3 + k_4 + k_5)\rho - \left(2 - k_3^2\right)\tilde{\eta},\end{aligned} \tag{15}$$

where $u \triangleq (u_i)_{i\in\mathcal{V}} \in \mathbb{R}^{nN}$, $\hat{\eta} \triangleq (\hat{\eta}_i)_{i\in\mathcal{V}} \in \mathbb{R}^{nN}$, $\hat{\zeta} \triangleq (\hat{\zeta}_i)_{i\in\mathcal{V}} \in \mathbb{R}^{nN}$, $\rho \triangleq (\rho_i)_{i\in\mathcal{V}} \in \mathbb{R}^{nN}$, and $\tilde{\eta} \triangleq (\tilde{\eta}_i)_{i\in\mathcal{V}} \in \mathbb{R}^{nN}$. Substituting (9)-(12) and (15) into the time-derivative of (11) yields

$$\dot{\tilde{r}} = (k_3 + k_4)\rho - \tilde{\eta} - \mathcal{H}(G(q_0, \dot{q}_0, t) - F(q, \dot{q}, t)) - k_4\tilde{r}, \tag{16}$$

where $G(q_0, \dot{q}_0, t) \triangleq (1_N \otimes g(q_0, \dot{q}_0, t)) \in \mathbb{R}^{nN}$, $F(q, \dot{q}, t) \triangleq (f_i(q_i, \dot{q}_i, t))_{i\in\mathcal{V}} \in \mathbb{R}^{nN}$, $q \triangleq (q_i)_{i\in\mathcal{V}} \in \mathbb{R}^{nN}$, and $\tilde{r} \triangleq (\tilde{r}_i)_{i\in\mathcal{V}} \in \mathbb{R}^{nN}$.

B. Distributed Controller Development

Based on the subsequent analysis, we design the distributed controller as

$$u_i = k_1k_2\eta_i + k_2\hat{\zeta}_i + k_2k_3\tilde{\eta}_i + k_2\rho_i, \tag{17}$$

where $k_2 \in \mathbb{R}_{>0}$ is a user-defined gain. Substituting (8), (9), and (11) into (17) yields

$$u = k_2\mathcal{H}r + k_2\tilde{r}. \tag{18}$$

Substituting (1), (2), (4), (5), and (18) into the time-derivative of (5) yields

$$\dot{r} = G(q_0, \dot{q}_0, t) - F(q, \dot{q}, t) - k_2\mathcal{H}r - k_2\tilde{r} + k_1r - k_1^2e. \tag{19}$$

The block diagramatic representation for a combined implementation of the distributed filter, observer, and controller is shown in Figure 1. The following section provides the stability analysis for the distributed filter, observer, and controller. To facilitate the stability analysis, we introduce the following lemma.

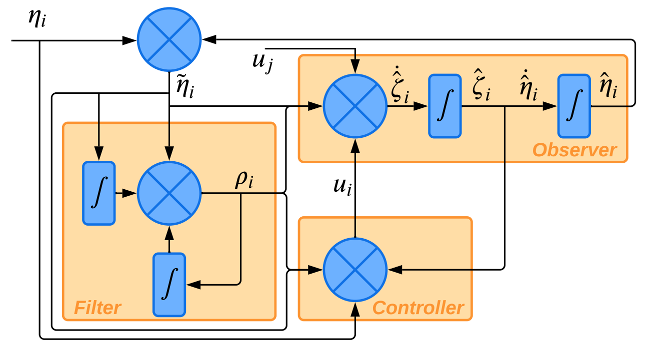

Fig. 1. Block diagram of algorithm implementation for agent $i \in \mathcal{V}$. Control gains have been omitted for clarity.

Lemma 1: Let $L \in \mathbb{R}_{\geq 0}$ be defined as $L \triangleq \max\{L_1, \ldots, L_N\}$, where $L_i \in \mathbb{R}_{\geq 0}$ is the drift Lipschitz constant for agent $i \in \mathcal{V}$ defined for $q, Q_0 \in \mathcal{D}_1 \subseteq \mathbb{R}^{nN}$ and $\dot{q}, \dot{Q}_0 \in \mathcal{D}_2 \subseteq \mathbb{R}^{nN}$, where $Q_0 \triangleq 1_N \otimes q_0 \in \mathbb{R}^{nN}$. There exists some constant $K \in \mathbb{R}_{\geq 0}$ such that

$$\|G(q_0, \dot{q}_0, t) - F(q, \dot{q}, t)\| \leq L\|r\| + L(1 + k_1)\|e\| + NK. \tag{20}$$

Proof: Adding and subtracting $F(q_0, \dot{q}_0, t)$ to $G(q_0, \dot{q}_0, t) - F(q, \dot{q}, t)$ and using the triangle inequality yields

$$\begin{aligned}\|G(q_0, \dot{q}_0, t) - F(q, \dot{q}, t)\| &\leq \|F\big(Q_0, \dot{Q}_0, t\big) - F(q, \dot{q}, t)\|\\ &\quad + \|G(q_0, \dot{q}_0, t) - F\big(Q_0, \dot{Q}_0, t\big)\|.\end{aligned} \tag{21}$$

Since g and f are continuous functions on $\mathcal{D}_1$ and $\mathcal{D}_2$, there exists some constant $K \in \mathbb{R}_{\geq 0}$ such that

$$\max_{i\in\mathcal{V}}\|g(q_0, \dot{q}_0, t) - f_i(q_0, \dot{q}_0, t)\| \leq K, \tag{22}$$

for all $t \in \mathbb{R}^n$. Applying (22) and the Lipschitz property of f_i, $\forall i \in \mathcal{V}$ to (21), and using the definitions of e and $\dot{e}$ yields

$$\|G(q_0, \dot{q}_0, t) - F(q, \dot{q}, t)\| \leq L(\|e\| + \|\dot{e}\|) + NK. \tag{23}$$

Substituting (5) into (23) and bounding the resulting inequality yields (20). ■

V. Stability Analysis

Define the state vector $\xi : \mathbb{R}_{\geq 0} \to \mathbb{R}^{5nN}$ as $\xi \triangleq [\,e^\top\ \ r^\top\ \ \tilde{\eta}^\top\ \ \tilde{r}^\top\ \ \rho^\top\,]^\top$. Using (5), (11), (12), (16), and (19) yields the closed-loop error system

$$\dot{\xi} = \begin{bmatrix} r - k_1e \\ G(q_0, \dot{q}_0, t) - F(q, \dot{q}, t) - k_2\mathcal{H}r - k_2\tilde{r} + k_1r - k_1^2e \\ \tilde{r} - k_3\tilde{\eta} - \rho \\ (k_3 + k_4)\rho - \tilde{\eta} - \mathcal{H}(G(q_0, \dot{q}_0, t) - F(q, \dot{q}, t)) - k_4\tilde{r} \\ \tilde{\eta} - (k_3 + k_4)\tilde{r} - k_5\rho \end{bmatrix}. \tag{24}$$

Consider the continuously differentiable Lyapunov function candidate $V : \mathbb{R}^{5nN} \to \mathbb{R}_{\geq 0}$ defined as

$$V(\xi) \triangleq \frac{1}{2}\xi^\top\xi. \tag{25}$$

Let $\gamma, \delta \in \mathbb{R}_{>0}$ be defined as $\gamma \triangleq \lambda_{\max}(\mathcal{L}_\mathcal{G}) + 1$ and $\delta \triangleq \frac{NK^2(1+\gamma)}{2}$, respectively.

Since the local Lipschitz property of F holds over a subset of $\mathbb{R}^{nN}$, the subsequent stability analysis requires ensuring $q \in \mathcal{D}_1$ and $\dot{q} \in \mathcal{D}_2, \forall i \in \mathcal{V}, \forall t \in \mathbb{R}_{\geq 0}$. This is achieved by yielding a local stability result which constrains the states as $\|\xi\| \leq \chi$, where $\chi \in \mathbb{R}_{>0}$. Based on the subsequent stability analysis, we define $\mathcal{S} \triangleq \{\varrho : \|\varrho\| \leq \sqrt{\chi^2 - \frac{\delta}{k}}\}$, where $k \in \mathbb{R}_{>0}$.

Theorem 1: Consider the dynamical systems described by (1) and (2). For any initial conditions of the states $\|\xi(t_0)\| \in \mathcal{S}$, the filter given by (13), observer given by (15), and controller given by (17) guarantee that there exists a constant k such that

$$\|\xi(t)\| \leq \sqrt{\left(\|\xi(t_0)\|^2 - \frac{\delta}{k}\right)\mathrm{e}^{-2k(t-t_0)} + \frac{\delta}{k}} \tag{26}$$

$\forall t \in [t_0, \infty)$, provided that the control gains k_1, k_2, and k_4 are selected such that $k_1 > 1$, $-\kappa_1(1 - k_1^2) - L(1 + k_1)(1 + \gamma) + 2k_1 > 0$, $k_2 > \frac{-k_1^2 + \kappa_1(k_1(2+L) + L(3+\gamma) + N) + 1}{\kappa_1(2\lambda_{\min}(\mathcal{H}) - \kappa_2)}$, and $k_4 > \frac{k_2 + \gamma\kappa_2(L(2+k_1)+N)}{2\kappa_2}$, where $\kappa_1 > 0$ and $\kappa_2 > 2\lambda_{\min}(\mathcal{H})$ are constants.[1]

Proof: Substituting (24) into the time-derivative of (25) yields

$$\begin{aligned}\dot{V}(\xi) = &-k_1 e^\top e - k_2 r^\top \mathcal{H} r - k_3 \tilde{\eta}^\top \tilde{\eta} - k_4 \tilde{r}^\top \tilde{r} - k_5 \rho^\top \rho \\ &+ k_1 r^\top r + \left(1 - k_1^2\right) e^\top r - k_2 r^\top \tilde{r} \\ &- \tilde{r}^\top (\mathcal{H}(G(q_0, \dot{q}_0, t) - F(q, \dot{q}, t))) \\ &+ r^\top (G(q_0, \dot{q}_0, t) - F(q, \dot{q}, t)).\end{aligned} \tag{27}$$

Applying Young's inequality to $(1 - k_1^2)e^\top r$ yields

$$\left(1 - k_1^2\right) e^\top r \leq \frac{\kappa_1 |1 - k_1^2|}{2}\|e\|^2 + \frac{|1 - k_1^2|}{2\kappa_1}\|r\|^2, \tag{28}$$

where $\kappa_1 \in \mathbb{R}_{>0}$. Similarly, we have that $-k_2 r^\top \tilde{r}$ may be upper bounded as

$$-k_2 r^\top \tilde{r} \leq \frac{k_2 \kappa_2}{2}\|r\|^2 + \frac{k_2}{2\kappa_2}\|\tilde{r}\|^2, \tag{29}$$

where $\kappa_2 \in \mathbb{R}_{>0}$. We can upper bound $r^\top (G(q_0, \dot{q}_0, t) - F(q, \dot{q}, t))$ by applying Lemma 1 as

$$\begin{aligned}r^\top (G(q_0, \dot{q}_0, t) - F(q, \dot{q}, t)) \leq &\frac{L(1 + k_1)}{2}\|e\|^2 \\ &+ \frac{L(3 + k_1) + N}{2}\|r\|^2 + \frac{NK^2}{2}.\end{aligned} \tag{30}$$

Based on the definition of the graph Laplacian, we can upper-bound the norm of $\mathcal{H}$ as

$$\|\mathcal{H}\|_2 \leq \gamma. \tag{31}$$

Similarly, we can upper bound $-\tilde{r}^\top (\mathcal{H}(G(q_0, \dot{q}_0, t) - F(q, \dot{q}, t)))$ by using (31), applying Lemma 1, and using Young's inequality, yielding

$$\begin{aligned}&-\tilde{r}^\top (\mathcal{H}(G(q_0, \dot{q}_0, t) - F(q, \dot{q}, t))) \\ &\leq \gamma \Bigg(\frac{L}{2}\|r\|^2 + \frac{L(1 + k_1)}{2}\|e\|^2 + \frac{L(2 + k_1) + N}{2}\|\tilde{r}\|^2 \\ &\quad + \frac{NK^2}{2}\Bigg)\end{aligned} \tag{32}$$

[1] By selecting gains to satisfy the inequalities sequentially, we ensure k's existence and positivity: a large k_1 for the quadratic, then a k_2 for its inequality, and a large k_4 for the final one.

Thus, we may upper bound (27) as

$$\dot{V}(\xi) \leq -k\|\xi\|^2 + \frac{NK^2(1 + \gamma)}{2}, \tag{33}$$

by using (28)-(30), (32), and invoking the gain conditions of k_1, k_2, and k_4. Using (25), we can upper bound (33) as

$$\dot{V}(\xi) \leq -2kV(\xi) + \delta. \tag{34}$$

Solving the differential inequality in (34) yields (26).

Further upper bounding the right side of (26) yields $\|\xi(t)\| \leq \sqrt{\|\xi(t_0)\|^2 + \frac{\delta}{k}}$ for all $t \in \mathbb{R}_{\geq 0}$. Consider the set $\bar{\mathcal{B}}_\chi \triangleq \{\iota : \|\iota\| \leq \chi\}$. If $\xi(t_0) \in \mathcal{S}$, then $\sqrt{\|\xi(t_0)\|^2 + \frac{\delta}{k}} \leq \chi$ which implies that $\xi \in \bar{\mathcal{B}}_\chi$ always holds. Since $\|\xi(t)\| \leq \chi$ implies $\|e\|, \|r\| \leq \chi$, the relations $\|q\| \leq \chi + N\bar{q}_0$ and $\|\dot{q}\| \leq (1 + k_1)\chi + N\bar{\dot{q}}_0$ hold. Thus, selecting χ such that $\mathcal{D}_1 = \{\iota_1 : \iota_1 \leq \chi + N\bar{q}_0\}$ and $\mathcal{D}_2 = \{\iota_2 : \iota_2 \leq (1 + k_1)\chi + N\bar{\dot{q}}_0\}$ ensures that $q \in \mathcal{D}_1$ and $\dot{q} \in \mathcal{D}_2$ for all $t \in \mathbb{R}_{\geq 0}$, thus always satisfying the local Lipschitz property. If F is globally Lipschitz, then the stability result holds for all initial conditions.

Similarly, since $\|\rho\|, \|\tilde{\eta}\|, \|\tilde{r}\| \leq \chi$, $\rho, \tilde{\eta}, \tilde{r} \in \mathcal{L}_\infty$. Thus, using (11) yields $\tilde{\zeta} \in \mathcal{L}_\infty$. Since $e, r \in \mathcal{L}_\infty$, using (5) yields $\dot{e} \in \mathcal{L}_\infty$. Since $e, \dot{e} \in \mathcal{L}_\infty$, using (8) and (9) yields $\eta, \zeta \in \mathcal{L}_\infty$. Since $\eta, \tilde{\eta}, \zeta, \tilde{\zeta} \in \mathcal{L}_\infty$, using (10) yields $\hat{\eta}, \hat{\zeta} \in \mathcal{L}_\infty$. Since $\eta_i, \hat{\zeta}_i, \tilde{\eta}_i, \rho_i \in \mathcal{L}_\infty$, using (17) yields $u \in \mathcal{L}_\infty$. Since $u, \rho, \tilde{\eta}, \hat{\zeta} \in \mathcal{L}_\infty$, using (15) yields $\dot{\hat{\zeta}}, \dot{\hat{\eta}} \in \mathcal{L}_\infty$. Therefore, all implemented signals are bounded. ∎

VI. Simulation

The performance of the developed controller is demonstrated through comparative simulations, with the method in [17] as the baseline. The controller and observer in the baseline method are given by

$$\begin{aligned}u_i &= \sigma\eta_i + \sigma\hat{\zeta}_i, \\ \dot{\hat{\eta}}_i &= \hat{\zeta}_i - \ell\tilde{\eta}_i, \\ \dot{\hat{\zeta}}_i &= \sum_{j \in \mathcal{N}_i}\left(u_j - u_i\right) - b_i u_i - \ell^2\tilde{\eta}_i,\end{aligned} \tag{35}$$

where $\sigma, \ell \in \mathbb{R}_{>0}$ are control and observer gains, respectively. The baseline method was developed assuming the agent dynamics are homogeneous and identical to the target, i.e., $f_i = g$ for all agents $i \in \mathcal{V}$. The developed method does not rely on this assumption, and thus also accounts for heterogeneity in the dynamics. To demonstrate the efficacy of the developed method, six simulations are performed, with each simulation having a different degree of heterogeneity. Each simulation is performed for 60 seconds, where six agents are tasked with tracking a moving target. The drift dynamics for agent $i \in \mathcal{V}$ in (1) are defined as those of a damped and driven harmonic oscillator, given by [17, eq. 40]

$$f_i(q_i, \dot{q}_i, t) = -a_i \sin(q_i) - b_i\dot{q}_i + c_i\cos(d_i t). \tag{36}$$

To show how varying levels of heterogeneity impact the results, we choose the parameters a_i, b_i, c_i, d_i from the uniform distribution $U(0, \omega)$. In each simulation, we use different values of ω to create these ranges, i.e., $\omega \in$

$\{0, 2.5, 5, 7.5, 10, 1000\}$, where a broader range of these parameters (i.e., higher ω) suggests a more diverse set of dynamics that controlled agents might encounter. Additionally, all simulations were conducted with an additive measurement noise sampled from a Gaussian distribution with variance 0.5.

The initial conditions of the agents are selected so that they form an equilateral hexagon of radius 0.5, centered at $(x, y, z) = (0.5, 0.5, 0)$. The dynamics for the target are also given by (36), with initial conditions

$$x_0(0) = y_0(0) = z_0(0) = 0.5,$$
$$\dot{x}_0(0) = \dot{y}_0(0) = 0, \dot{z}_0(0) = 0.1.$$

Three agents are selected so that $b_i = 1$, with the remaining three agents having $b_i = 0$, i.e., only three agents could measure the relative positions between themselves and the target. This configuration results in the indicator matrix being given by $\mathrm{diag}(0, 1, 0, 1, 0, 1)$. The graph Laplacian for the network is given by

$$\mathcal{L}_{\mathcal{G}} = \begin{bmatrix} 3 & 0 & -1 & -1 & -1 & 0 \\ 0 & 3 & 0 & -1 & -1 & -1 \\ -1 & 0 & 3 & 0 & -1 & -1 \\ -1 & -1 & 0 & 3 & 0 & -1 \\ -1 & -1 & -1 & 0 & 3 & 0 \\ 0 & -1 & -1 & -1 & 0 & 3 \end{bmatrix}.$$

An adaptive Monte-Carlo method is used to select the final gains in each simulation. A total of 25,000 trials are run for each value of ω, with the gains being selected from the uniform distribution $U(0.001, 50)$. The cost function is defined as

$$J = \int_0^{t_f} \left(\|e(t)\|^2 + \tau^2 \|\tilde{\zeta}(t)\|^2 \right) \mathrm{d}t,$$

where $\tau = 0.25$ is a scaling factor.

Every 1000 trials, the top 50% performing trials are selected and the corresponding gains are used to determine the new set for random gain initialization. To ensure a fair comparison, both scenarios employ the same adaptive Monte Carlo simulation approach, and all the initial conditions, dynamics, and simulation parameters for both agents and targets are kept identical. The simulations are ran in parallel to ensure that the random dynamic parameters are identical for both simulations. The final gains selected for the both the developed controller and the baseline controller are shown in Table I.

Considering the limitations of the baseline method outlined in [17] for heterogeneous scenarios, we conducted a homogeneous comparison ($\omega = 0$), the results of which are depicted in Figure 2. These results validate the efficacy of our method even in the absence of heterogeneity. To further test our methods effectiveness, we increased ω up to 1000. As shown in Table I, our controller maintains satisfactory tracking performance without significant degradation, even under high heterogeneity levels.

Figure 3 shows the tracking errors using our developed method at $\omega = 2.5$, with Table II listing the corresponding randomly initialized parameters. As evident from Figure 3, all agents effectively track the target with $\|e_i\| < 0.1$ after approximately 0.5 seconds.

TABLE I
RESULT COMPARISON

ω	Method	Gains	Error	$\|e\|^2$	$\|\tilde{\zeta}\|^2$
0	Developed	39.35, 10.24, 4.01, 1.05, 41.25	RMS	0.04	0.87
			Max	0.70	5.47
	Baseline	36.21, 5.20	RMS	0.11	0.87
			Max	0.71	5.47
2.5	Developed	37.45, 14.34, 3.17, 2.51, 39.29	RMS	0.04	1.32
			Max	0.70	13.37
	Baseline	35.23, 6.91	RMS	0.42	1.50
			Max	0.91	10.32
5.0	Developed	30.62, 22.11, 0.34, 8.94, 31.43	RMS	0.03	1.24
			Max	0.70	17.70
	Baseline	35.11, 13.11	RMS	0.23	1.15
			Max	0.71	20.00
7.5	Developed	18.97, 22.39, 0.13, 16.21, 11.45	RMS	0.04	1.52
			Max	0.70	25.94
	Baseline	34.53, 14.42	RMS	0.18	1.50
			Max	0.71	22.44
10	Developed	9.75, 32.41, 0.05, 20.28, 23.45	RMS	0.06	1.78
			Max	0.70	32.65
	Baseline	34.63, 16.45	RMS	0.18	1.80
			Max	0.70	22.93
1000	Developed	9.75, 32.41, 0.05, 20.28, 23.45	RMS	0.31	14.13
			Max	0.94	37.95
	Baseline	34.63, 16.45	RMS	Unstable	
			Max	Unstable	

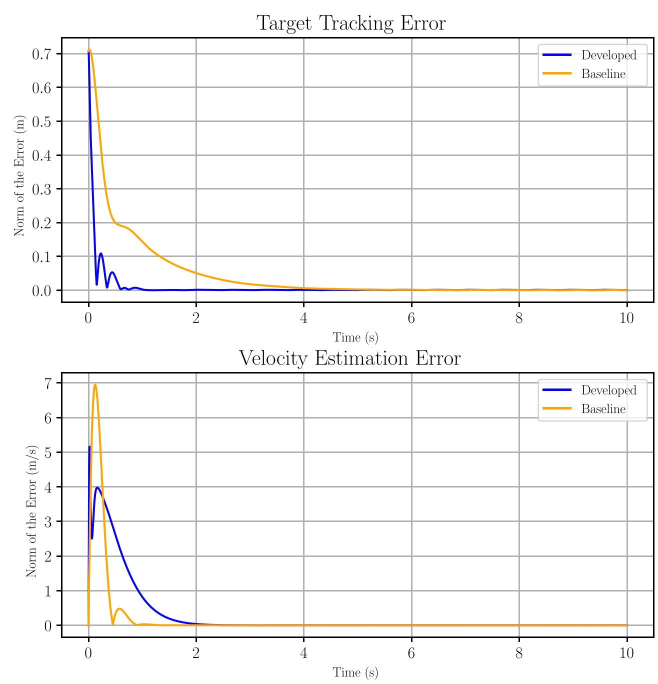

Fig. 2. Plots of the tracking and velocity estimation errors for the homogeneous comparison ($\omega = 0$).

Table I provides the Root Mean Square (RMS) and maximum tracking and velocity estimation errors for the six simulations using both developed and baseline methods. The baseline method shows a performance decline with increasing dynamics heterogeneity (i.e., higher ω) in contrast to the developed method. Particularly at $\omega = 10$, the developed method significantly outperforms the baseline method, as shown in Figure 4, achieving a 67% improvement in the RMS tracking error.

Fig. 3. Plot of the tracking errors for each agent, when the dynamic parameters a_i, b_i, c_i, d_i are selected from the uniform distribution $U(0, 2.5)$.

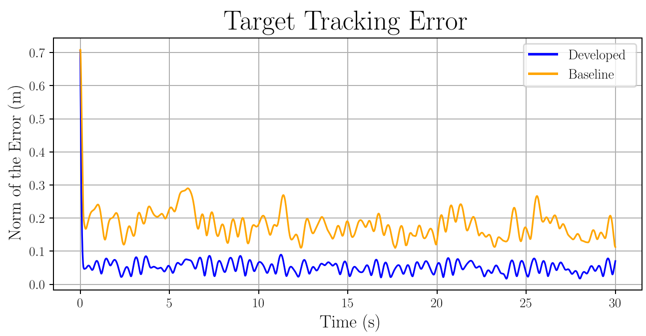

Fig. 4. Comparative plots of the average tracking errors, when the dynamic parameters a_i, b_i, c_i, d_i are selected from the uniform distribution $U(0, 10)$.

TABLE II
HETEROGENEITY PARAMETERS FOR $\omega = 2.5$

Agent	$a = (a_x, a_y, a_z)$ / $c = (c_x, c_y, c_z)$	$b = (b_x, b_y, b_z)$ / $d = (d_x, d_y, d_z)$
Agent 1	2.27, 1.33, 1.86	0.91, 1.86 ,1.76
	0.46, 1.96, 0.55	0.46, 1.96, 0.55
Agent 2	0.26, 1.07, 0.87	0.70, 1.27, 0.92
	0.88, 1.36, 0.63	1.14, 0.06, 0.87
Agent 3	1.33, 2.34, 0.88	1.10, 1.42, 1.45
	2.42, 0.95, 2.24	1.00, 0.81, 0.07
Agent 4	0.56, 0.83, 2.40	0.82, 1.44, 1.39
	1.21, 2.36, 0.82	2.35, 1.14, 2.19
Agent 5	1.77, 1.97, 2.40	2.28, 2.25, 0.29
	1.38, 1.52, 0.99	1.82, 2.40, 2.17
Agent 6	2.17, 2.17, 1.36	1.80, 1.34, 0.98
	0.91, 1.51, 1.53	1.52, 1.37, 2.34
Target	0.23, 2.08, 0.88	0.93, 2.35, 1.92
	1.67, 1.76, 0.25	1.82, 1.84, 2.36

VII. CONCLUSION

This letter develops an approach to address the distributed target tracking problem in the context of heterogeneous second-order multi-agent systems by developing a novel distributed observer based on a distributed filter. The distributed observer and filter enable the network of agents to estimate the velocities of all agents as well as the target, and achieve network-to-target regulation. A Lyapunov-based stability analysis is used to guarantee that all agents are exponentially regulated to a neighborhood of the target. Simulations are provided to demonstrate the performance of the developed distributed controller. The developed method provides a 67% improvement in the RMS tracking error, when compared to the baseline method in [17]. Future efforts could explore the use of adaptive control methods to approximate the uncertain agent dynamics to reduce the conservative gain conditions of the developed approach.

ACKNOWLEDGMENT

Any opinions, findings and conclusions or recommendations expressed in this material are those of the authors and do not necessarily reflect the views of the sponsoring agency.

REFERENCES

[1] R. Yang, L. Liu, and G. Feng, "An overview of recent advances in distributed coordination of multi-agent systems," *Unmanned Syst.*, vol. 10, no. 3, pp. 307–325, Jul. 2022.
[2] G. Chen and F. L. Lewis, "Distributed adaptive tracking control for synchronization of unknown networked Lagrangian systems," *IEEE Trans. Syst., Man, Cybern., Syst.*, vol. 41, no. 3, pp. 805–816, Jun. 2011.
[3] Y. Bouteraa, J. Ghommam, G. Poisson, and N. Derbel, "Distributed synchronization control to trajectory tracking of multiple robot manipulators," *J. Robot*, vol. 2011, Aug. 2011, Art. no. 652785.
[4] B. Zhu, H. H.-T. Liu, and Z. Li, "Robust distributed attitude synchronization of multiple three-DOF experimental helicopters," *Control Eng. Pract.*, vol. 36, pp. 87–99, Mar. 2015.
[5] T. Chen and J. Shan, "Distributed spacecraft attitude tracking and synchronization under directed graphs," *Aerosp. Sci. Technol.*, vol. 109, Feb. 2021, Art. no. 106432. [Online]. Available: https://www.sciencedirect.com/science/article/pii/S1270963820311147
[6] D. V. Dimarogonas, P. Tsiotras, and K. J. Kyriakopoulos, "Leader–follower cooperative attitude control of multiple rigid bodies," *Syst. Control Lett.*, vol. 58, no. 6, pp. 429–435, 2009.
[7] S. Li, H. Du, and X. Lin, "Finite-time consensus algorithm for multi-agent systems with double-integrator dynamics," *Automatica*, vol. 47, no. 8, pp. 1706–1712, 2011. [Online]. Available: https://www.sciencedirect.com/science/article/pii/S0005109811001464
[8] I.-L. G. Borlaug, K. Y. Pettersen, and J. T. Gravdahl, "Comparison of two second-order sliding mode control algorithms for an articulated intervention AUV: Theory and experimental results," *Ocean Eng.*, vol. 222, Feb. 2021, Art. no. 108480. [Online]. Available: https://www.sciencedirect.com/science/article/pii/S0029801820313871
[9] Y. Hong, J. Hu, and L. Gao, "Tracking control for multi-agent consensus with an active leader and variable topology," *Automatica*, vol. 42, no. 7, pp. 1177–1182, 2006.
[10] S. Liu, D. Tan, and G. Liu, "Robust leader–follower formation control of mobile robots based on a second order kinematics model," *Acta Automatica Sinica*, vol. 33, no. 9, pp. 947–955, 2007.
[11] Y. Hong, G. R. Chen, and L. Bushnell, "Distributed observers design for leader following control of multi-agent networks," *Automatica*, vol. 44, no. 3, pp. 846–850, 2008.
[12] W. Ren, "On consensus algorithms for double-integrator dynamics," *IEEE Trans. Autom. Control*, vol. 53, no. 6, pp. 1503–1509, Jul. 2008.
[13] Y. Gao, L. Wang, and Y. Jia, "Consensus of multiple second-order agents without velocity measurements," in *Proc. Amer. Control Conf.*, 2009, pp. 4464–4469.
[14] J. Hu and G. Feng, "Distributed tracking control of leader–follower multi-agent systems under noisy measurement," *Automatica*, vol. 46, no. 8, pp. 1382–1387, 2010.
[15] H. Kim, H. Shim, and J. H. Seo, "Output consensus of heterogeneous uncertain linear multi-agent systems," *IEEE Trans. Autom. Control*, vol. 56, no. 1, pp. 200–206, Jan. 2011.
[16] Y. Zheng and L. Wang, "Consensus of heterogeneous multi-agent systems without velocity measurements," *Int. J. Control*, vol. 85, no. 7, pp. 906–914, 2012.
[17] H. Du, Y. Cheng, Y. He, and R. Jia, "Second-order consensus for nonlinear leader-following multi-agent systems via dynamic output feedback control," *Int. J. Robust Nonlinear Control*, vol. 26, no. 2, pp. 329–344, Feb. 2015.
[18] C. Qian and W. Lin, "Output feedback control of a class of nonlinear systems: A nonseparation principle paradigm," *IEEE Trans. Autom. Control*, vol. 47, no. 10, pp. 1710–1715, Oct. 2002.
[19] Z. Qu, *Cooperative Control of Dynamical Systems: Applications to Autonomous Vehicles*. London, U.K.: Springer-Verlag, 2009.